

**DESIGN OF AN ORIGAMI-INSPIRED VARIABLE STIFFNESS
WRIST BRACE**

A Thesis Presented

by

Mengtao Zhao

To

The Department of Mechanical and Industrial Engineering

in partial fulfillment of the requirements

for the degree of

Master of Science

in

Mechanical Engineering

Northeastern University

Boston, Massachusetts

June 2018

ABSTRACT

Carpal tunnel syndrome is a nerve disorder that afflicts 5% of the U.S. population. Treatment often includes wearing a rigid brace to immobilize the wrist, but this brace is not comfortable and can limit mobility. We propose an active wearable device that can alter its stiffness while being worn, transforming from a mechanically transparent, comfortable state to a rigid, protective one in seconds. To realize this, we present the design, modeling, and fabrication of an origami-inspired variable stiffness element that alters its rigidity by folding and unfolding, and its integration into a wearable brace.

To understand and implement this approach, we develop and validate a model that predicts the element's rigidity as a function of material and geometric properties. We use a three-point bending test to characterize the effect of changing different materials and fold patterns on the element's stiffness in both the 'rigid' and 'flexible' states, as well as the ratio between the two. We select one design to incorporate into our brace, and show it has a stiffness ratio between these two modes of 38.5 in theoretical mode and 20.8 in the final model.

To integrate the origami-inspired variable-stiffness element into a wearable machine, we developed an anchoring approach to mechanically join the variable-stiffness element to a soft glove, and a tendon-driven system that can repeatably actuate folding and unfolding in a low-power and practical design. We further will characterize how these elements impact the effective stiffness of the brace in resisting wrist movement.

Keywords: Wrist Brace, Origami, Variable-Stiffness, Stiffness Ratio

ACKNOWLEDGEMENTS

I would first like to thank my thesis advisor Prof. Samuel Felton. The door to Prof.Felton office was always open whenever I ran into a trouble spot or had a question about my research or writing. He consistently allowed this paper to be my own work and steered me in the right the direction.

I would like to thank my workmate on this research, Marcos Batista Oliveira, for sharing his experience and helping solve many problems along the way. I would also like to thank all the members of the lab for their assistance, and especially Chang Liu, Akshay Vaidya and Mutian Fan.

I would also like to acknowledge Prof. Rifat Sipahi and Dr.Philip Long as the second reader of this thesis, and I am gratefully indebted to their very valuable comments on this thesis.

Finally, I must express my very profound gratitude to my parents and girlfriend for providing me with unfailing support and continuous encouragement throughout my study and through the process of researching and writing this thesis. This accomplishment would not have been possible without them. Thank you.

List of Contents

1 Introduction	1
1.1 Introduction and Problem Statement	1
1.2 Background	3
1.2.1 Research of Pneumatic Operated Splint	4
1.2.2 Variable Impedance Exoskeleton Based on Hydraulic Actuation.....	5
1.3 Variable-Stiffness Structures	6
1.3.1 Mechanical Based Approach	6
1.3.2 Material Based Approach	7
1.3.3 Geometrical Based Approach	8
2 Design and Fabrication	10
2.1 Fabrication and Mechanical Test	10
2.1.1 Design and Fabrication Process	10
2.1.2 Three-point bending Test.....	12
2.2 Pattern Comparison.....	13
2.3 Material Comparison	16
2.4 Wrist Brace Assembly	19
2.5 Wrist Movement with Wrist Brace	21
3 Modeling and Analysis	21
3.1 Modeling	21
3.2 Model Validation	23
3.3 Integrated Brace Testing	27
4 Discussion	28
REFERENCES	30

List of Figures

Figure 1: V-groove radiator model [2].....	1
Figure 2: Solar array in open (left) and close (right) states [3].....	2
Figure 3: Carpal tunnel syndrome [7].....	3
Figure 4: ASSIST configuration in flat mode and bending mode [8].....	4
Figure 5: Working principle for NEUROExos [10]	5
Figure 6: AwAS working principle [11].....	7
Figure 7: (a) Developed snake-like manipulator including three linear actuators. (b) Closed up view of tubular shape with a large hollow space [14]	8
Figure 8: Hinged structure in flat and corrugated mode.....	9
Figure 9: Integrated wrist brace	10
Figure 10: Views of hinged structure (a) Features on the top plate (b) Features on the bottom plate (c) The cross section of the hinged structure after cutting the extra edges	10
Figure 11: Fabrication process. (1) Fix the top plate on baseboard by alignment rods (2) Lay down the double-sided tape (3) Stick the nylon film on the top plate (4) Cut holes on nylon film (5) Lay down another layer double-side tape (6) Stick the bottom layer (7) Cut the extra edges by laser machine (8) Get the final model.....	12
Figure 12: Three-point-bending test. The left one is in flat mode. The right one is in corrugated mode.....	13
Figure 13: Three various pattern named after their basic element which are rectangle, Miura and corrugated features.....	14
Figure 14: The loading curve in three-point bending for corrugated pattern hinged structure. The shadow region represents the variation of different samples and the vertex of nylon material is 311.9 N.....	15
Figure 15: The loading curve in three-point bending for rectangle pattern hinged structure. The shadow region represents the variation of different samples and the vertex of nylon material is 22.48 N.....	15
Figure 16: The loading curve in three-point bending for Miura pattern hinged structure. The shadow region represents the variation of different samples and the vertex of nylon material is 12.51 N.....	16

Figure 17: Three-point-bending test for different materials in flat mode and corrugated mode, (1) and (2) are made of Nylon 6/6, (3) and (4) are made of polystyrene, (5) and (6) are made of steel	17
Figure 18: Three-point bending test in corrugated position, where the green line is nylon, the orange line is steel and the blue line is polystyrene. The shadow region shows the variation of different samples.....	18
Figure 19: Three-point bending test for flat position, where the green line is nylon, the orange line is steel and the blue line is polystyrene. The shadow region shows the variation of different samples.....	18
Figure 20: The hinged structure with elastic bands, thread, motor and motor bracket.....	20
Figure 21: Motor and connector (1) shows the simulated model, (2) and (3) show the views of real model.....	20
Figure 22: Wrist movement with wrist brace	21
Figure 23: Cross section of flat mode and corrugation mode	22
Figure 24: Bending modulus sample	24
Figure 25: Hinged structure A	24
Figure 26: Hinged structure B.....	25
Figure 27: Hinged structure C.....	25
Figure 28: Hinged structure D	26
Figure 29: Integrated wrist brace test.....	27
Figure 30: Torque exerted against the wrist brace as a function of angular deflection in both the flat mode and corrugated mode [17].....	28

List of tables

Table 1: Fabrication materials	11
Table 2: Hinged structure comparison.....	26

1 Introduction

1.1 Introduction and Problem Statement

Origami is an art developed in Japan which transforms a flat sheet into designed shapes by various folding techniques. In the modern world, origami technology has played an important part in mechanical engineering due to its multifunctional, economical, and space saving features. This technology has been applied in many fields, such as space technology, architecture and medical devices.

In space technology, NASA engineers have designed numerous pieces of hardware, offering scientists opportunities to pack large structures in small packages. For example, the Wide Field Infrared Survey Telescope (WFIRST) is composed of many small pieces capable of folding and unfolding [1]. This origami design enables the telescope to change its shape and size to avoid micrometeorite strikes.

Another example is a radiator that can fold and unfold, much like V-groove paper structure (Figure 1) created with origami [2]. The advanced design of a three-dimensional, foldable radiator can control the rate of heat by changing shape. This geometrical changing could be achieved with shape memory alloys. The radiator could automatically change its shape to either shed or conserve heat corresponding to the angle it faces the sun.



Figure 1: V-groove radiator model [2]

Another origami design provides a novel way to design a solar array [3]. A technique called the Miura fold is used for the solar array, which allows the array to open evenly into a checkerboard of the parallelogram. With this particular fold, there is only one way to open or close it: Pull on one corner and then the whole thing is open with minimal effort. The mechanical structure of a device that folds this way is greatly simplified because only one input is required to deploy.(Figure 2)



Figure 2: Solar array in open (left) and close (right) states [3]

In architecture, origami technology has been used to save energy and adjust light exposure [4]. For example, walls and windows can change shape and transparency to control the light intake of buildings according to the changing weather. Furthermore, this origami design can absorb and release heat inside in buildings to regulate temperature efficiently.

Origami technology also plays a significant part in the development of medical devices, such as wrist braces and back orthopedic devices. This thesis focuses on the medical rehabilitation device on wrist brace, which improves symptoms of carpal tunnel syndrome (CTS).

Carpal tunnel syndrome (CTS) is a common entrapment neuropathy that affects wrists and hands. It usually happens due to the compression of the median nerve when it passes the wrist at the carpal tunnel [5]. The patients experience numbness and pain in their fingers and wrists, and such symptoms usually increase at night. As time progresses, such pain will gradually spread to

the whole arm, which will cause weak grip and wrist shape change. There is evidence that people who tend to have CTS symptoms are overweight, pregnant or people who conduct repetitive wrist work, such as computer work, work with vibrating tools, or works that need large grip strength. About 5% of people in the United States are afflicted with carpal tunnel syndrome [6]. Thus, to develop possible rehabilitation method for such patients are not only necessary but also crucial.

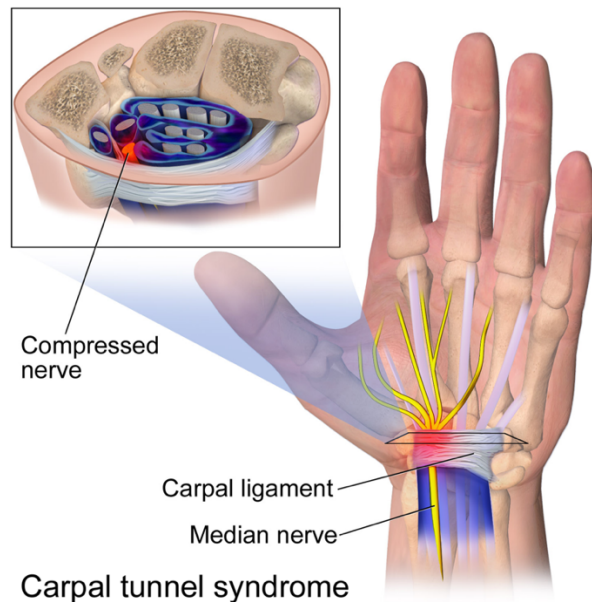


Figure 3: Carpal tunnel syndrome [7]

Currently, one of the most useful medical treatments for CTS is the wrist splint [6]. However, the flexible wrist braces that are commonly used in daily life have little effect to improve symptoms and the fixed wrist splint design usually impedes daily movement of users. In this thesis, we propose an origami wrist brace to help patients with more flexibility.

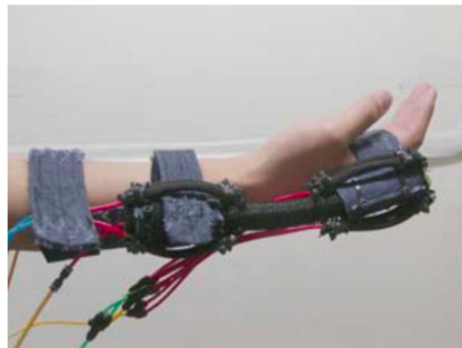
1.2 Background

In the domain of wearable devices, especially those with variable stiffness machine, engineers are always trying to find a balance between flexibility and rigidity. For example, soft and breathable wearable machines let patients feel comfortable, but a stiff medical plasterboard is able to protect the users from an accidental collision. To better balance these two characteristics, engineers have come up with many devices with the capability to change stiffness, such as

pneumatic operator splints, soft exosuits and worm robots. Some examples of wrist healing devices are listed below.

1.2.1 Research of Pneumatic Operated Splint

Researchers at Okayama University has developed a wearable machine named ASSIST to assist those who have weak grip strength [8]. Engineers in this team utilized McKibben type pneumatic rubber muscles as actuators to generate force and torque, in order to bend users' wrists [9]. Actuators like these can be operated through air pressure which causes the actuator to contract or extend. After having it assembled it with straps and appliance, this wrist brace is able to assist the users' wrist to move.



(a) Initial state



(b) Pressurized state

Figure 4: ASSIST configuration in flat mode and bending mode [8]

As shown in figure 4, the actuator has a rubber tube in the middle attached by two silicone rubber tubes on the upper and bottom sides with polyester. The equipment has three layers of bonding tubes with the polyester attached below, which guide the movement of the rubber tube during operation. By injecting compressed air into the actuator, the tube will bend from the side

with that polyester to the other side without polyester. After sewing with other parts, this equipment can produce about 20 N force.

The advantages of this device can be summarized: First, it is lightweight and users can easily put it on. Second, the fabrication of this device is simple, and it is convenient for users to modify with accessories.

However, there are some drawbacks. First, its strength is limited due to individual fibers, and it also has limited moving space because of the tightness of the weave. Second, it uses an external compressor as the power source to activate the whole system, which means users can only wear it in a particular place with a bulky air pump.

1.2.2 Variable Impedance Exoskeleton Based on Hydraulic Actuation

Another elbow and wrist exoskeleton with variable impedances was developed to assist patients' rehabilitation in stroke and CTS [10]. It uses hydraulic cylinders as a power supply to control the movement of an exoskeleton.

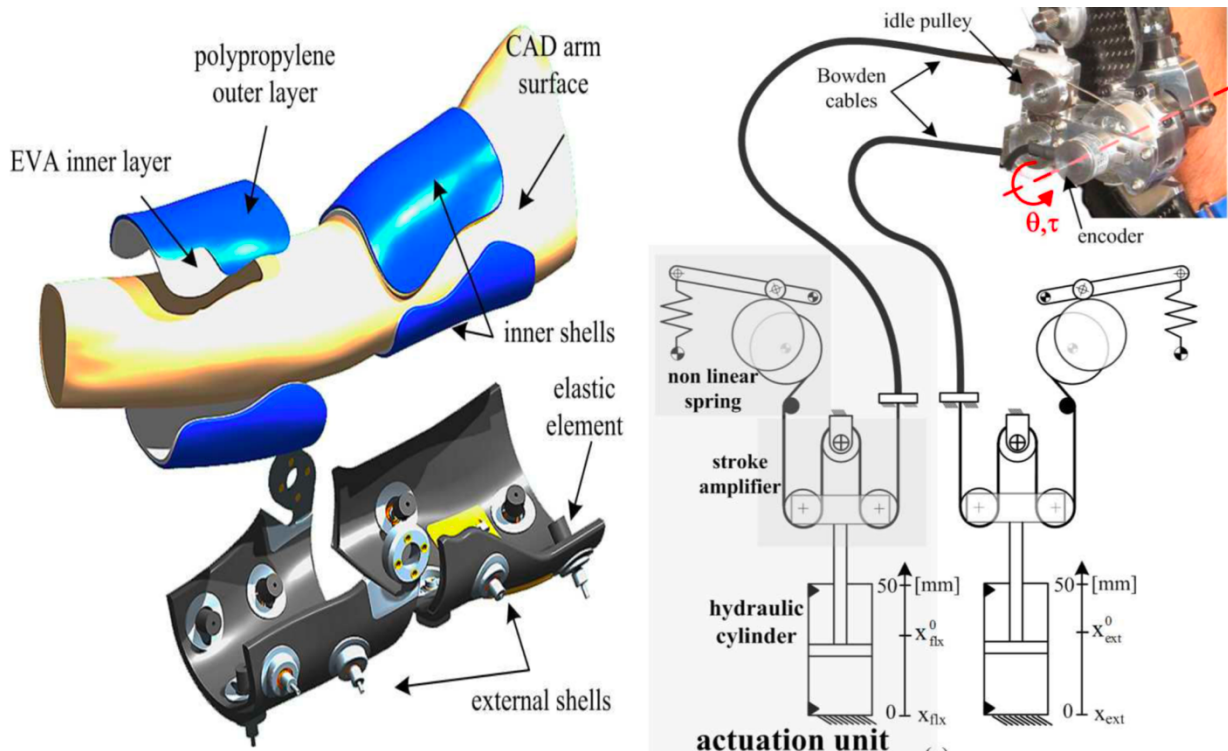


Figure 5: Working principle for NEUROExos [10]

As shown in Figure 5, the researchers developed a double-shell link structure to fix the users' forearm, which consists of an inner shell and elastic external shells. The inner shell, made of soft polypropylene, provides wearability and comfort to the human wrist, and reduces the force on user's skin to reduce pains from pressure. As for the outer shell, it provides support to the users' arm and was connected to the actuated unit through a driving block with a Bowden cable. The embedded sensors can transfer the moving signals to the control system, which can regulate the joint axis to stick with the instantaneous human joint rotation. The bio-inspired actuated unit can control the joint's stiffness and position in an open-loop fashion. In this way, it is able to transfer required joint torque with a low output impedance among the frequency range of possible inputs.

This design provides an example of an upper limb exoskeleton design and provides inspiration for the protection of users' skin. Its doubled-shell structure with hydraulic actuation also offers a reliable solution for capturing human behaviors with corresponding adjustments. However, due to the size of the hydraulic cylinders, this equipment is only applicable in specific places like hospital and medical center, and the power efficiency is lower which may cause environmental issues. In addition, the fabrication is costly and time-consuming and the device is very bulky.

1.3 Variable-Stiffness Structures

In order to change the stiffness of a variable stiffness structure, there are three methods which are the mechanical based approach, material-based approach and geometrical based approach [11].

1.3.1 Mechanical Based Approach

A mechanical system can change its stiffness by changing its boundary condition to which it subjects to. For example, a lever arm can change its stiffness by adjusting the length of its arm. Other examples include changing the position of the pivot point, the spring point and force application. These all can be applied to the joint rotation in a robotic application. For example, Dr. Jafari has developed a mechanical arm (AwAS) with adjustable stiffness [12]. As Figure 6 shows, it is capable of controlling the joint stiffness with minimum energy by regulating the position of the arm levels and springs in the system.

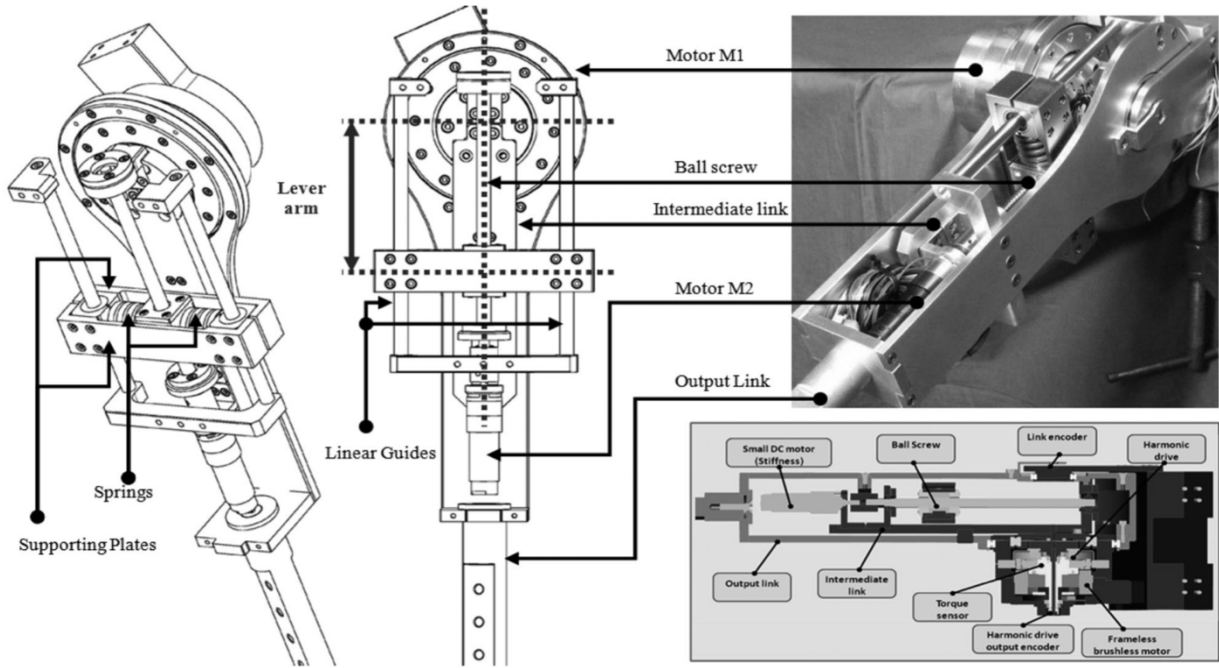


Figure 6: AwAS working principle [11]

1.3.2 Material Based Approach

The mechanical system can also adjust the elastic properties of the whole structure by altering the elastic material properties or the internal interaction between its structural components.

Proposed approaches with the direct change in the mechanical properties are phase transition [13] and glass transition [14]. The elastic properties can be modified by heat, chemical reaction or electromagnetic field. For example, Dr. Yong-Jae Kim developed a novel snake-like manipulator [15]. As shown in Figure 7, it used layer jamming technology to change the shape of the robot and change the stiffness with the application of a vacuum. By changing part of the robot property through layer jamming, this robot can bend and move during the operation.

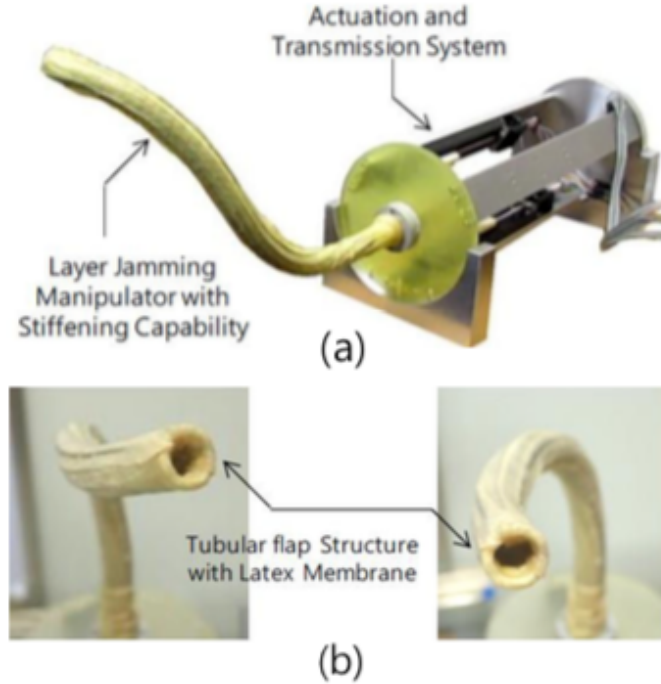


Figure 7: (a) Developed snake-like manipulator including three linear actuators. (b) Closed up view of tubular shape with a large hollow space [14]

1.3.3 Geometrical Based Approach

The geometrical based approach can change the shape and the cross section configuration to affect the second moment of area of the whole system. This modification can lead to an increase or a decrease of the bending stiffness of the structure while keeping the material properties. In this classification, the dimension of the whole structure will be modified based on several effects, such as folding mechanisms, shape memory effect, or pneumatic expansion [11].

In this thesis, we are going to use a folding mechanism to create a significant change in bending stiffness by altering the cross section geometry (Figure 8). It allows the possibility of building an economic wrist brace associated with changeable stiffness and can be used in the medical treatment of CTS to immobilize users' wrists.

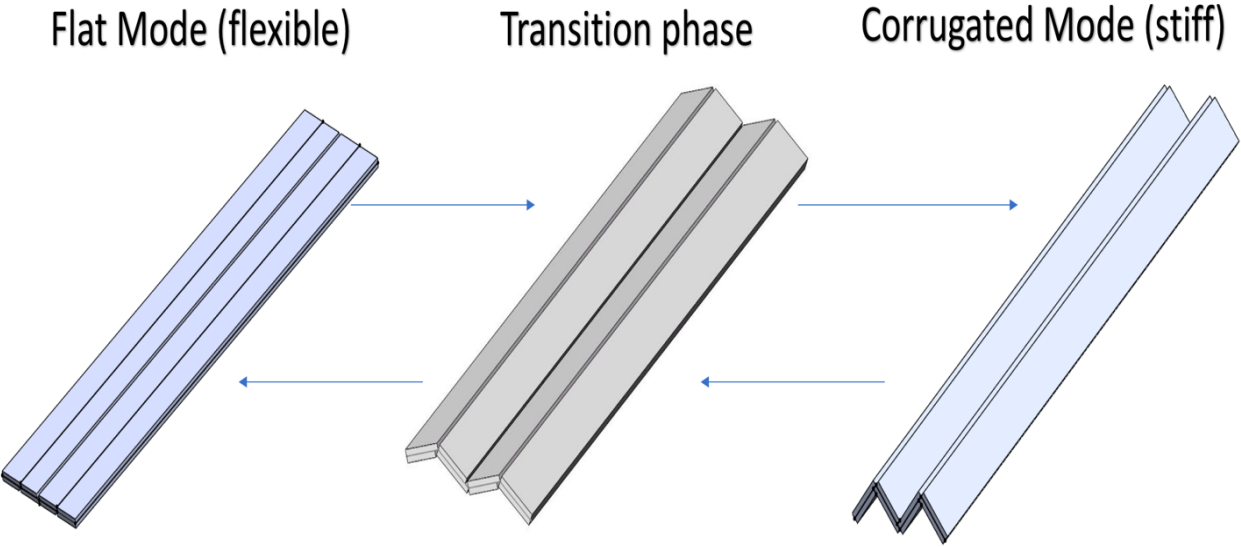


Figure 8: Hinged structure in flat and corrugated mode

As shown in Figure 9, the wrist brace consists of a glove, a hinged structure, a motor and a constraining strap. The glove is used to protect skin from the pain, the hinged structure attached with a spinning motor can provide changeable stiffness mechanism for wrist brace, and a rigid strap is used to constrain the hinged structure on the wrist.

The main component of the wrist brace is the hinged structure, which is a laminated structure consisting of a soft layer with two rigid outer layers. Gaps are cut in the rigid layers to allow the flexural layer to bend easily. These gaps are offset so that the rigid layer is able to interlock when it is folded, and the double-side tape is used to bond each layer. The basic method of the hinged structure to change stiffness is applying torsion to each beam. Therefore, a motor powered by batteries applies tension to a thread that drives transformation.

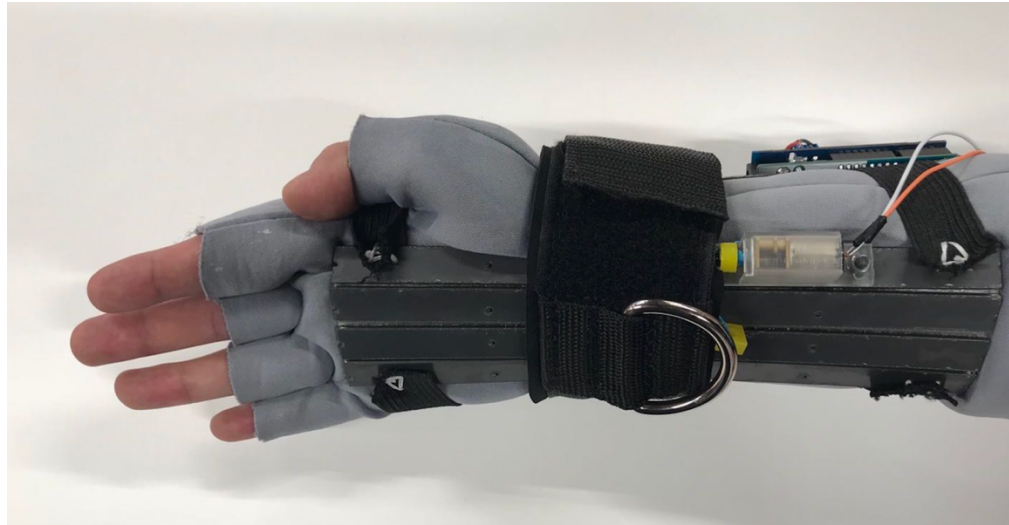


Figure 9: Integrated wrist brace

2 Design and Fabrication

2.1 Fabrication and Mechanical Test

To characterize the best design for the hinged structure, its parameters are varied to correspond to the mechanical performance. Analysis of these designs through three-point bending tests and wrist brace assembly are shown below.

2.1.1 Design and Fabrication Process

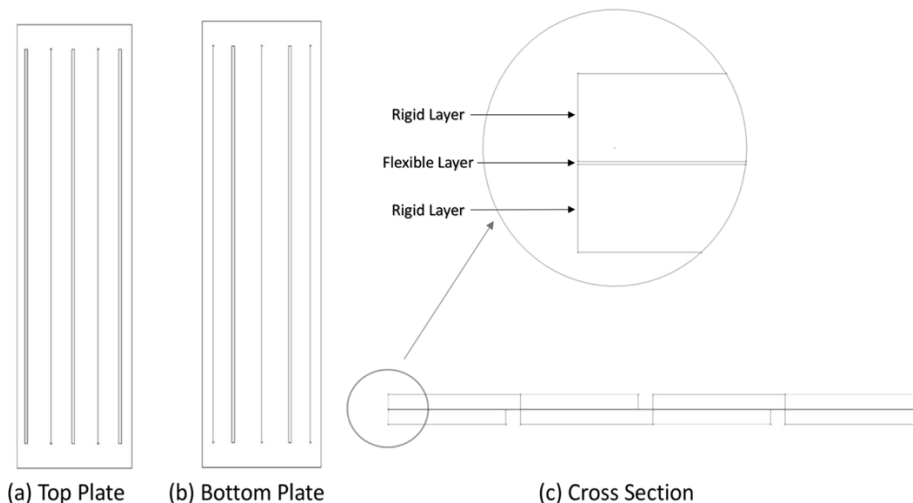


Figure 10: Views of hinged structure (a) Features on the top plate (b) Features on the bottom plate (c) The cross section of the hinged structure after cutting the extra edges

To design the hinged structure, some features of the rigid layers are drawn by SolidWorks in Figure 10. Each layer consists of six beams with specific gaps, and two extra parts at the edges to fix them in place. The two beams with shorter widths in the horizontal direction are 12.7 x 108 mm, which are used as the release parts to keep the constant of the gap and are removed after combining parts of the whole structure. The release parts also include two beams with shorter widths 6.35 mm in the longitude direction, which provide extra space to extended double-side tapes in the fabrication process. For the final model of the hinged structure, the dimensions of each layer are 203.2 x 108 x 1.6 mm and the gap is equal to the thickness of each layer.

After finishing the features on SolidWorks, a laser machine is used to cut the pattern. The materials and dimensions to build the hinged structure are shown in Table 1.

Table 1: Fabrication materials

	Dimension (mm)	Material
Upper layer	228.6 x 73 x 3.2	Nylon 6/6
Bottom layer	228.6 x 73 x 3.2	Nylon 6/6
Adhesive	228.6 x 73 x 3.2	Nylon film
Base plate	248 x 91 x 4.6	Acrylic

The fabrication steps are listed below and shown in Figure 11.

Step 1: Place the upper layer on the baseboard and hold in place by inserting four aluminum dowel pins to fix the baseboard.

Step 2: Lay down the double-sided tape on the upper layer with some margin in order to prevent the sheet from dislocating.

Step 3: Take out the pins and spread on a layer of nylon film, extruding bubbles from the clearance and press down for one minute.

Step 4: Use a knife to cut holes on the nylon film that correspond to sheet pattern, in order to use the aligning pins in the next steps.

Step 5-6: Put another layer of double-sided tape on the nylon film, press it for one minute and then apply another layer nylon sheet.

Step 7-8: For the purpose of separating the tabs, apply a release cut at each side of the sheet and then the structure is completed.

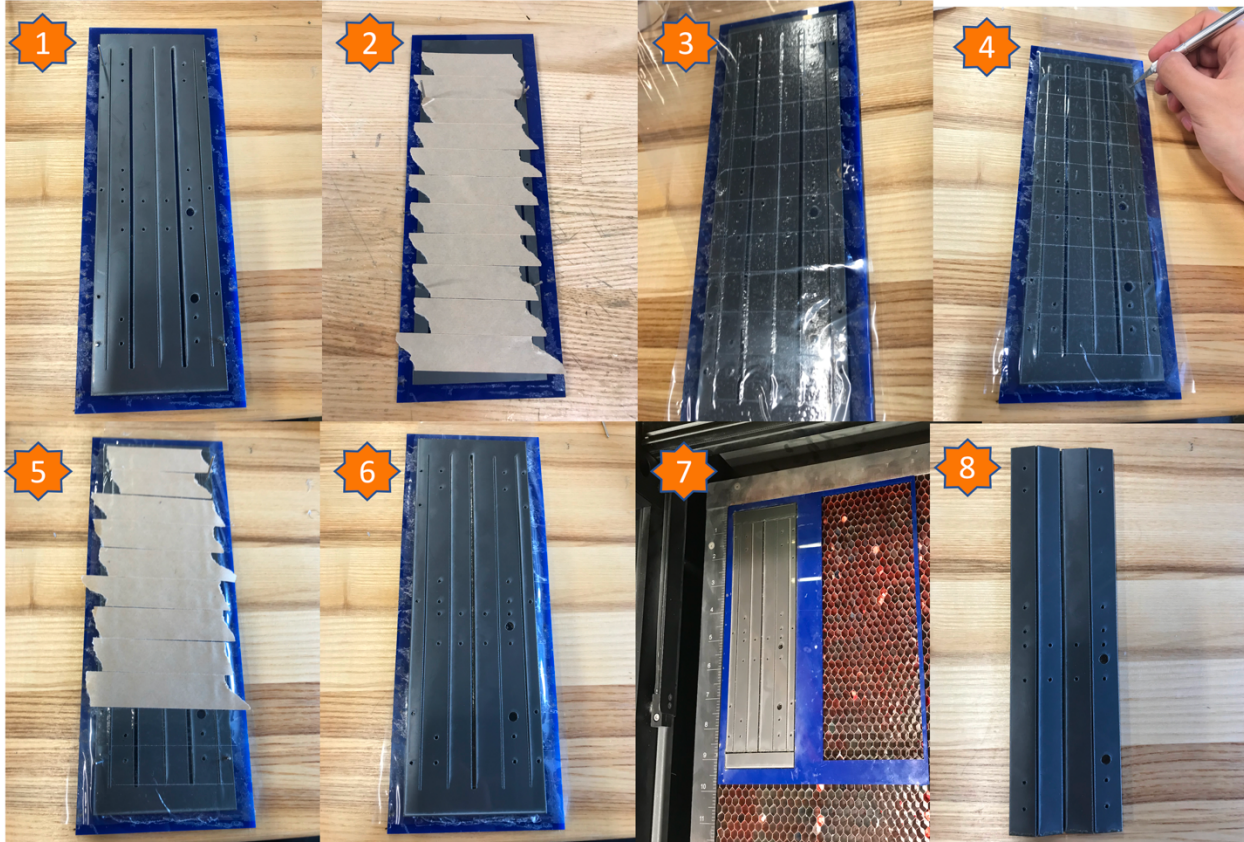


Figure 11: Fabrication process. (1) Fix the top plate on baseboard by alignment rods (2) Lay down the double-sided tape (3) Stick the nylon film on the top plate (4) Cut holes on nylon film (5) Lay down another layer double-side tape (6) Stick the bottom layer (7) Cut the extra edges by laser machine (8) Get the final model

2.1.2 Three-point bending Test

Three-point bending test is a useful method to measure the effective bending stiffness E . In these experiments, we used a multi-tester (Mecmesin Multi-Test 2.5i) with a 250 N load cell and a 2500 N load cell to test the bending stiffness of the hinged structure in flat and corrugated mode. The structure is simply supported at either end by two points that are 152.4 mm apart and in each experiment, the loading probe displaces 20 mm. Figure 12 shows the pressing process of the final model.

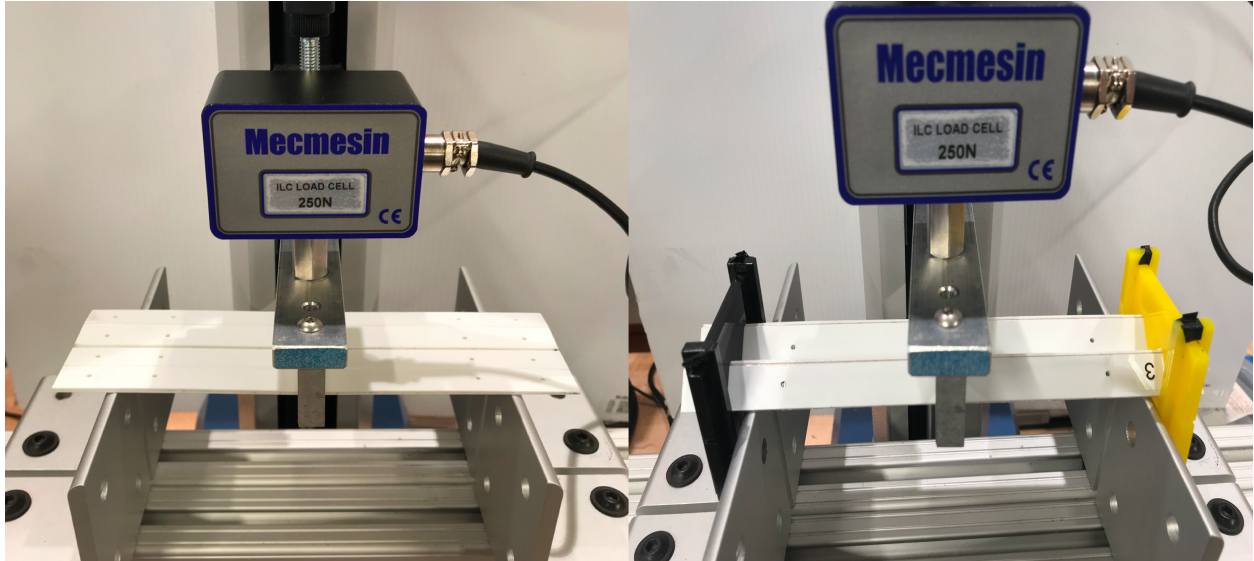


Figure 12: Three-point-bending test. The left one is in flat mode. The right one is in corrugated mode

2.2 Pattern Comparison

To find a suitable structure to build the hinged structure which is able to fix the human wrist, a set of compared tests with various patterns on rigid layers are designed. Nylon, a material with excellent mechanical property in hinged structure, is used to build samples. Besides, acrylic material, which has the high strength and the low toughness property, is used as a compared team to examine the bending stiffness of patterns.

Figure 13 shows three patterns in acrylic and nylon material which is named as rectangle, miura and corrugated for their shapes. Each model is made with two layers hinged structure with dimensions 254 x 81 x 3.2 mm. The results of the three-point-bending test are shown in figure 14-16.

For each rectangle element, each piece is 42.3 x 12.7 mm and there are 6 elements in horizontal direction and 8 elements in the vertical direction. The Miura piece is 42.3 x 18 mm and the angle between intersection line is 45 degrees. To fold these two hinged structures bidirectionally, each piece with odd number is 1.6 mm wider than even number. The dimension of each corrugated element is 254 x 12.7 mm in the odd number and 254 x 14.3 mm in even number. To align the two rigid layers, each piece has two holes to make room for alignment rods. To keep

the accuracy of the experiments, 2500 N load cell was used to test the corrugated pattern and 250 N load cell was used to test the rectangle and Miura pattern.

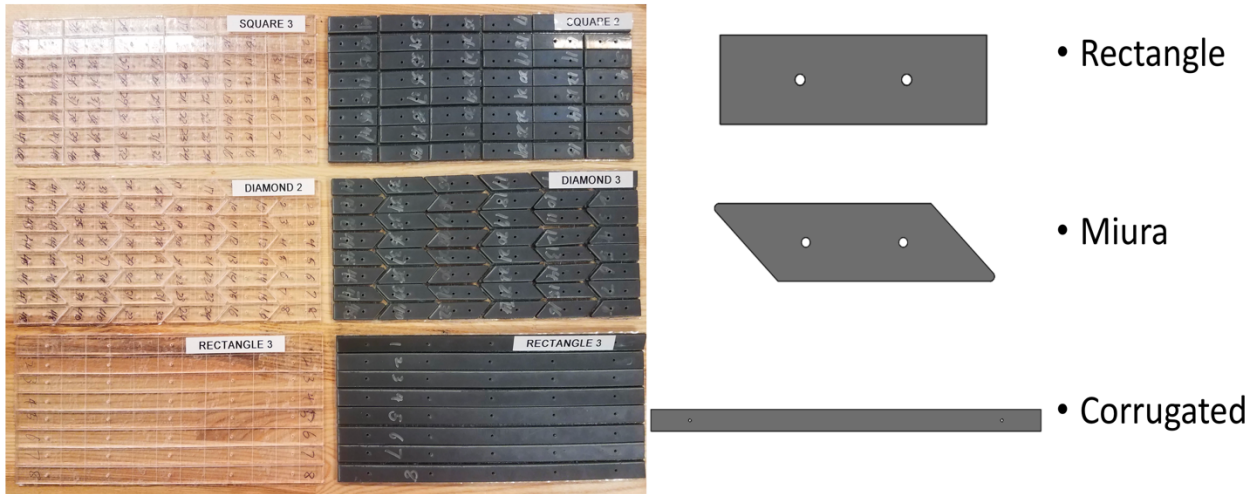


Figure 13: Three various patterns named after their basic element which are rectangle, Miura and corrugated features

As shown in Figure 12, a pair of light-weight clamps was used to fix the hinged structure in corrugated mode and was laid down between two supports. For flat mode, it was set naturally on the supports without any clamps or attachments.

Figure 14-16 shows the relationship between the displacement and the load, in which acrylic hinged structure is the red region and nylon hinged structure is the blue region. The rising part of the curve shows the process when load cell pressed on the hinged structure without deforming. And the declining part of the curve shows the part that the hinged structure deformed. Compared to rectangle pattern and Miura pattern whose vertex of the curve is 22.5 N and 12.5 N respectively, the vertex of corrugated pattern curve is 312 N, which is much higher than the other two patterns and suitable to build the hinged structure.

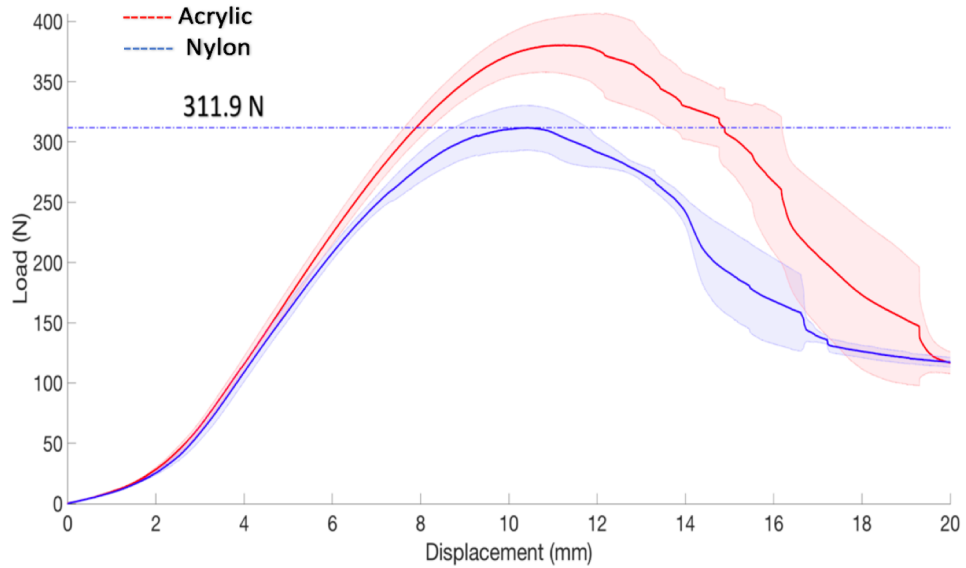


Figure 14: The loading curve in three-point bending for corrugated pattern hinged structure. The shadow region represents the variation of different samples and the vertex of nylon material is 311.9 N

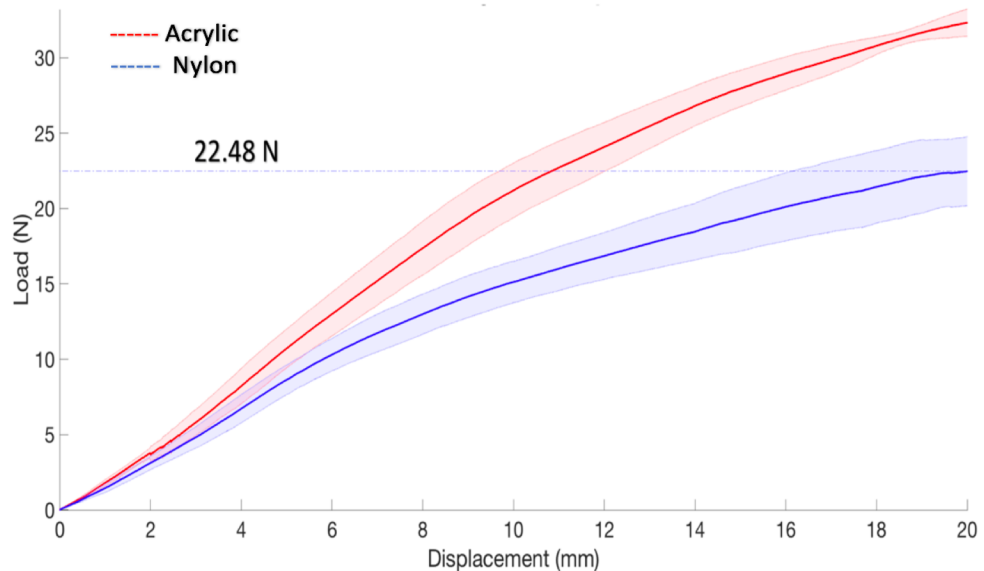


Figure 15: The loading curve in three-point bending for rectangle pattern hinged structure. The shadow region represents the variation of different samples and the vertex of nylon material is 22.48 N

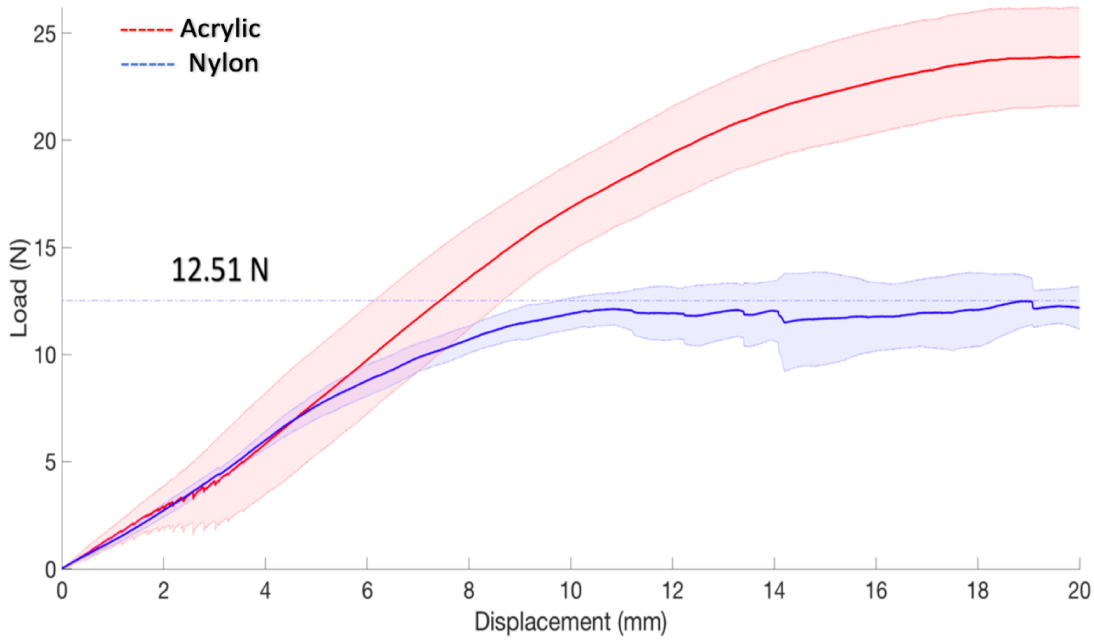


Figure 16: The loading curve in three-point bending for Miura pattern hinged structure. The shadow region represents the variation of different samples and the vertex of nylon material is 12.51 N

2.3 Material Comparison

After determining the pattern on the rigid layer, this section is going to select a material to build hinged structure. Three flexible materials are used in this experiment for their excellent mechanical property in origami research. They are nylon 6/6, polystyrene and steel shim. Because the thickness of steel the laser cutter able to cut is 0.15 mm, in these experiments, we used a 0.13 mm thickness steel shim. And to decrease the error of different thickness, nylon 6/6 and polystyrene are both 0.8 mm thickness, which is the thinnest sheet that could be bought in the market. Therefore, hinged structure dimensions in nylon and polystyrene are 203.2 x 60.2 x 0.8 mm and steel is 203.2 x 60.2 x 0.13 mm.

Three-point bending test was used to test the mechanical performance of the hinged structure in a different material (Figure 18). To ensure the accuracy of the load-displacement relation, 250 N load cell was used in these experiments and the results are shown in Figure 19-20.

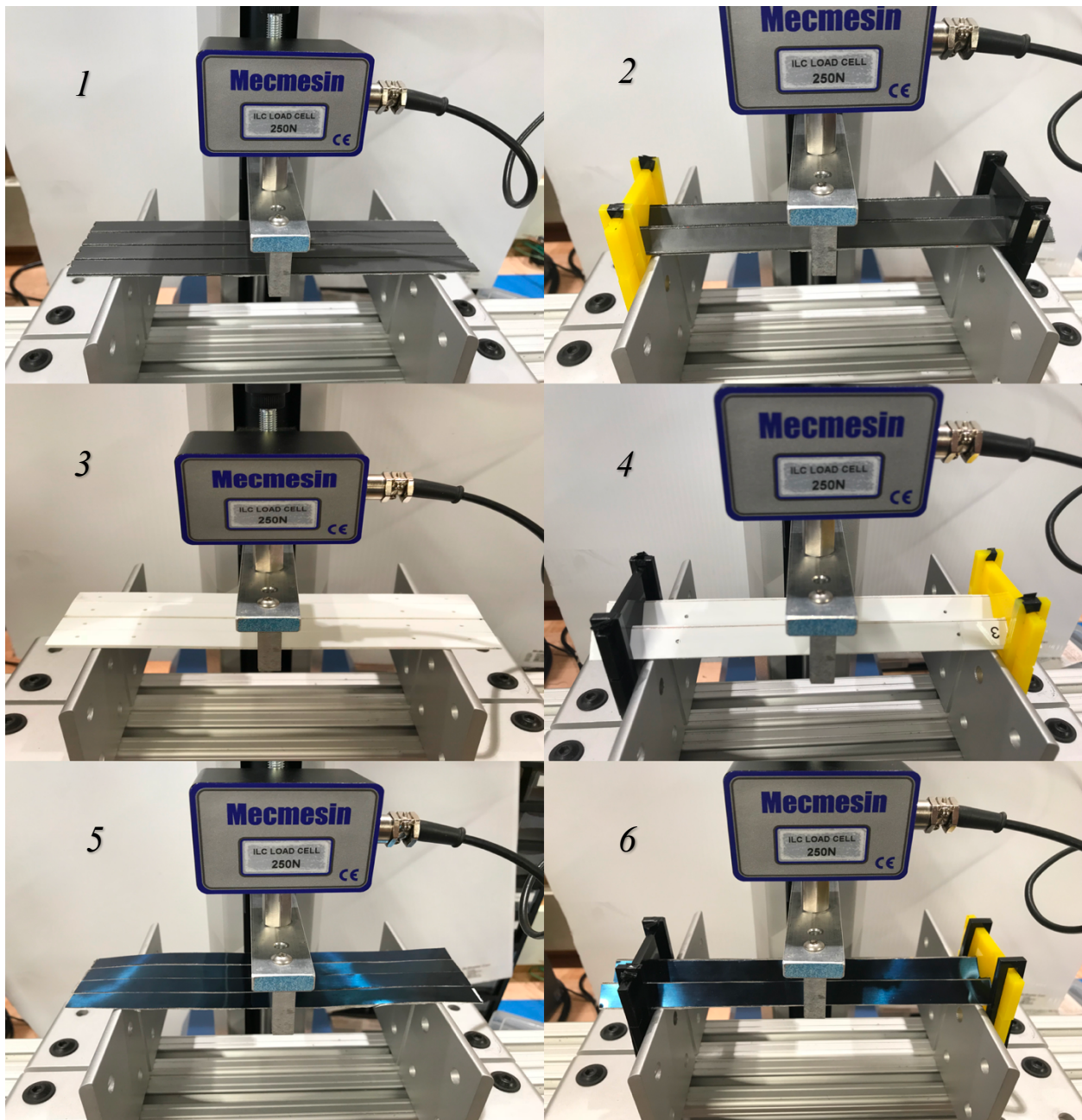


Figure 17: Three-point-bending test for different materials in flat mode and corrugated mode, (1) and (2) are made of Nylon 6/6, (3) and (4) are made of polystyrene, (5) and (6) are made of steel

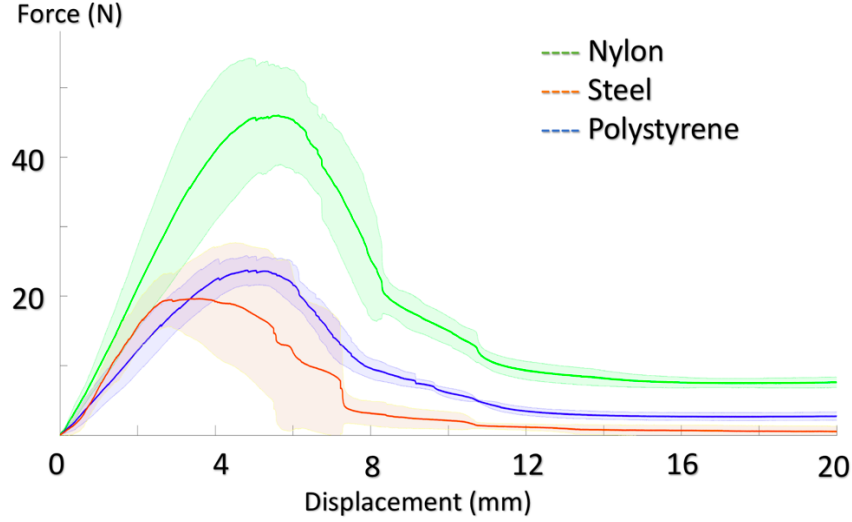


Figure 18: Three-point bending test in corrugated position, where the green line is nylon, the orange line is steel and the blue line is polystyrene. The shadow region shows the variation of different samples.

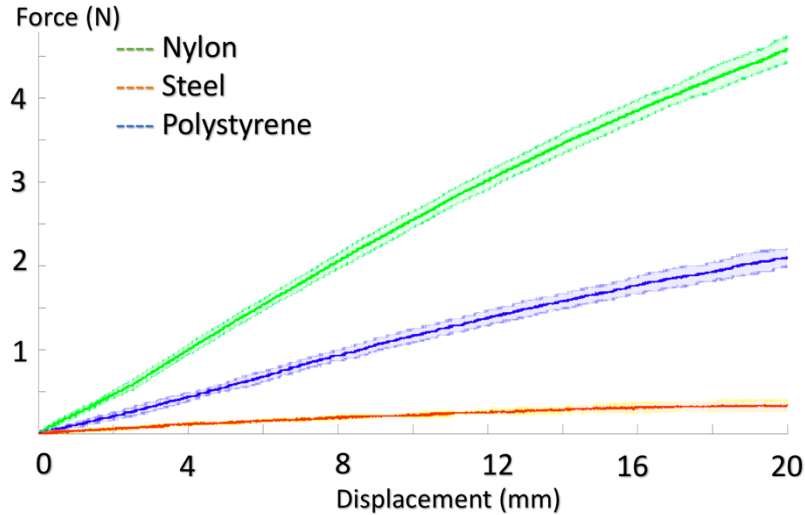


Figure 19: Three-point bending test for flat position, where the green line is nylon, the orange line is steel and the blue line is polystyrene. The shadow region shows the variation of different samples.

There are two standards used to judge the performance of mechanical property in corrugated structure. One is the maximum load the structure can hold and the other is the stiffness ratio. The maximum load represents the highest load a hinged structure can bear without deforming and the stiffness ratio represents the relation between the flexibility and rigidity of a hinged structure. Higher the maximum of a hinged structure, the better the mechanical property it is, and higher the stiffness ratio, the hinged structure performs better in the wrist brace. Both of them are supposed to be considered before deforming and the part after deforming will be discussed later.

As shown in Figure 19, the maximum load on the nylon hinged structure in corrugated mode is about (45 N), higher than polystyrene (22.5 N) and steel shim (19.6 N). According to calculation, the stiffness ratios of nylon, polystyrene and steel are 37, 45 and 325 respectively. Because these results, nylon 6/6 was finally chosen for the following three reasons. First, although the stiffness ratio of nylon 6/6 is lower than polystyrene and steel shim, it is able to hold more loads before structure deforming, and people can rotate their wrist easily in flat mode. Second, the sharp edge of steel is inclined to cut users' skin. Third, we could observe that the polystyrene hinged structure performed delamination during the bending process.

2.4 Wrist Brace Assembly

To complete an integrated human wrist, some designs are used to attach the actuation unit on the hinged structure in order to actuate the whole system (Figure 20).

First, to lock the hinged structure on users' wrist, elastic bands are sewed on the edge of hinged structure and to reduce the gap between the hinged structure and wrists, a constraining strap is used when users wear the wrist brace. As shown in Figure 26, The length of the bands located at the two edges is 127 mm and the middle one is 102 mm based on ergonomics. The triangle knots sewed on each band are used to prevent the longitudinal and lateral movement of bands on beams.

Second, a mini motor and a thread are taken into account for the design in order to provide force to change the hinged structure from flat mode to corrugated mode. The mini motor can provide $3.4 \text{ kg} * \text{m}$ torque to roll the thread on the shaft. A small connector is used to connect the thread and shaft (Figure 21). The connector has two holes, the larger one is used to lock the connector to shaft with instant, and small one allows the thread to pass through. The ends of the thread are fixed on the connector and hinged structure with two tying nods. Some holes on hinged structure are cut on beams that provide space for thread and elastic bands. The holes are chambered to reduce friction when the thread moving. When the motor rotates forward, it can wrap the thread on shaft and stretch the thread, which changes the configuration from flat mode to corrugated mode. And it also locks the hinged structure when the motor stops. Based on experiments, the

largest force to open the corrugated mode is about 30 N. When the motor rotates back, the thread would move back with the shrink of elastic bands. The hinged structure configuration would also return from corrugated mode to flat mode. A set of batteries is bonded on a small plate which is located on the other side of the wrist to power the whole system.

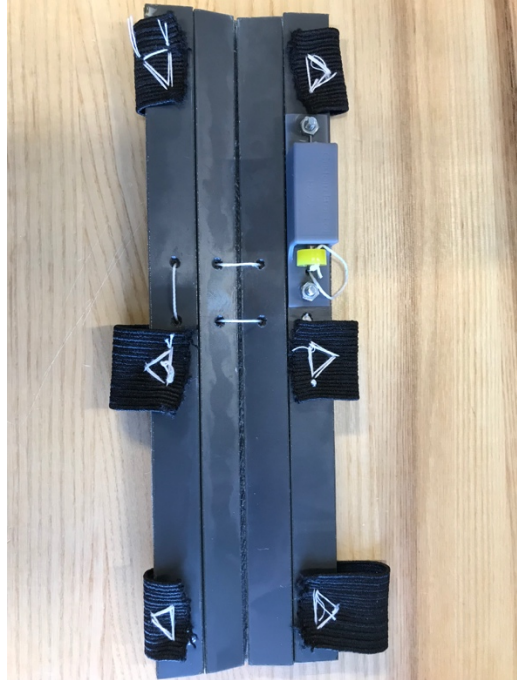


Figure 20: The hinged structure with elastic bands, thread, motor and motor bracket

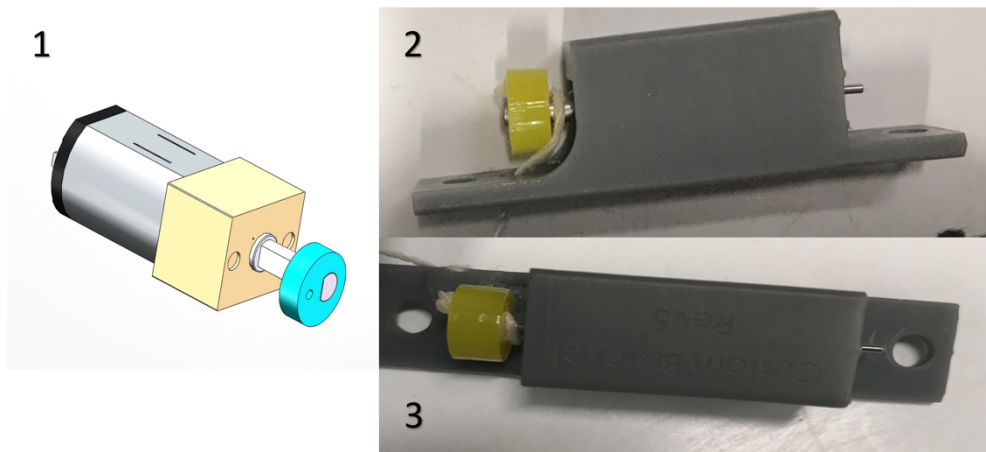


Figure 21: Motor and connector (1) shows the simulated model, (2) and (3) show the views of real model

2.5 Wrist Movement with Wrist Brace

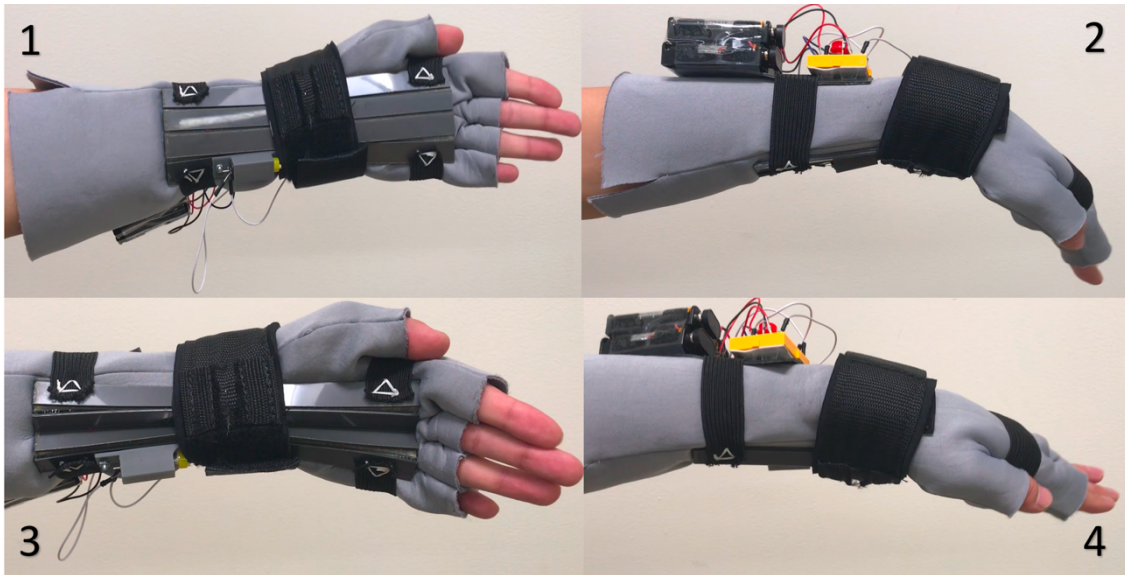


Figure 22: Wrist movement with wrist brace

Figure 22 shows the wrist movement with the brace, where picture (1)-(2) shows the movement in the flat mode and picture (3)-(4) shows movement in the corrugated mode. To protect skin from the sharp edges of the hinged structure, a glove made of neoprene was fabricated to cover most of forearm. Users can switch modes by pushing the button, which is located on back of wrist.

3 Modeling and Analysis

3.1 Modeling

To get a better understanding of the variable stiffness of the hinged structure, a model was derived to explain the specific relationship between the flat and corrugated modes. Generally, stiffness is the resistance to deformation in response to an applied force [16]. In the elastic bending region, the specific standards to judge the stiffness of the structure are the material bending modulus E and the second moment of area I . To capture the performance of the hinged structure, a three-point bending test was used and the exact pattern has been set as we talked before. Therefore, we are able to determine the equation of characteristic stiffness [16]:

$$k = \frac{48EI}{L_{eff}} \quad (1)$$

Where E is the bending modulus of the material, I is the second moment of area, and L_{eff} is the effective length between the two supports.

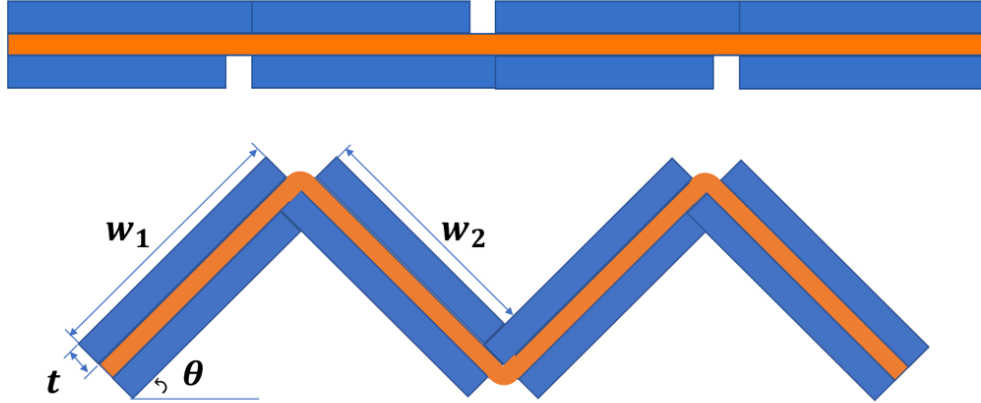


Figure 23: Cross section of flat mode and corrugation mode

To understand the structure of the laminated two-streak beams, figure 17 shows the cross sections of the hinged structure in the flat and corrugated modes respectively. Assuming this hinged structure consists of n beams bonded together, in which $\frac{n}{2} + 1$ beams have longer width w_1 , $\frac{n}{2} - 1$ beams have shorter width w_2 , the thickness of each beam is t , the angle of corrugation is θ and the thickness of the nylon film is $50 \mu\text{m}$. Based on equation 1, we can get the stiffness of flat and corrugated modes respectively, and then conclude the second moment of area ratio equals to the stiffness ratio in equation 2.

$$\frac{I_c}{I_f} = \frac{k_c}{k_f} \quad (2)$$

Where I_c and I_f are the second moment of area corresponding to the corrugated mode and flat mode and k_c and k_f correspond to the characteristic stiffnesses. Therefore, the equations in the flat and corrugated mode are shown below in equations 3 and 4.

$$I_c = \frac{w_1 t^3 (\frac{n}{2} + 1)}{12} + \frac{w_2 t^3 (\frac{n}{2} - 1)}{12} \quad (3)$$

$$\begin{aligned} I_f = & \frac{n}{4} \left(\frac{w_1 t^3 + t w_1^3}{12} + \left(\frac{w_1 t^3 - t w_1^3}{12} \right) x \cos(2\theta) \right) \\ & + \left(\frac{w_1 t^3 + t w_1^3}{24} + \left(\frac{w_1 t^3 - t w_1^3}{24} \right) x \cos(2\theta) + \frac{t^3 w_1^2}{4} \sin(2\theta) \right) \\ & + \frac{n}{4} \left(\frac{w_2 t^3 + t w_2^3}{12} + \left(\frac{w_2 t^3 - t w_2^3}{12} \right) x \cos(2\theta) \right) \\ & - \left(\frac{w_2 t^3 + t w_2^3}{24} + \left(\frac{w_2 t^3 - t w_2^3}{24} \right) x \cos(2\theta) + \frac{t^3 w_2^2}{4} \sin(2\theta) \right) \end{aligned} \quad (4)$$

In this model, torsion and shearing effect are not considered in the whole structure due to the complexity of the equation.

3.2 Model Validation

In order to experimentally validate the theoretical model, we conducted further experiments with nylon.

At first, the bending modulus E of nylon 6/6 requires to be tested, so we used 3-point bending test on the cuboid nylon 6/6 samples. The dimensions of the sample are 152.4 x 50.8 x 1.6 mm and the distance between the two supports is 101.6 mm. Using equation (1), we can get the bending modulus 3.24 Gpa. (Figure 24)

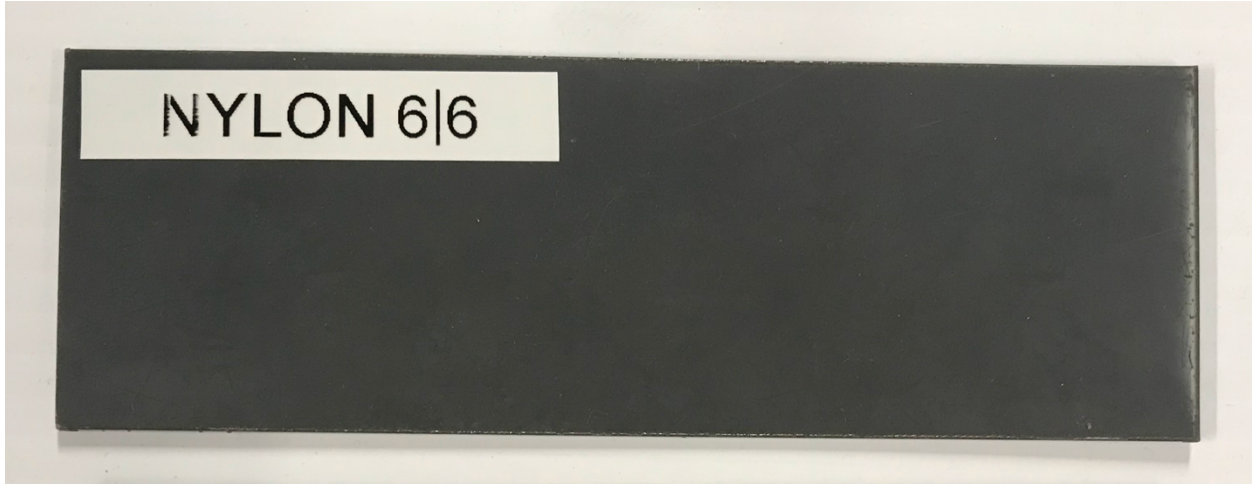


Figure 24: Bending modulus sample

Based on the analysis on the modeling, the bending stiffness of a hinged structure is determined by two parameters regarding to the corrugated pattern, which are bending modulus E , and second moment of area I . It depends on five geometric parameters, which are w_1, w_2, t, θ, n . Four candidates with different values of I (Table 2) were made to compare and the best one was selected. (Figure 25-28)

A

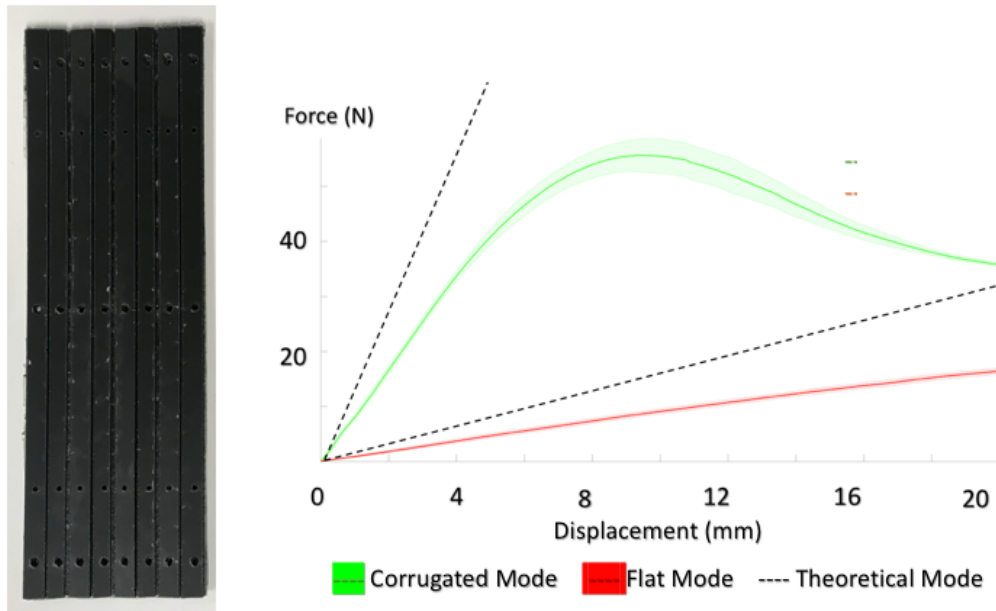


Figure 25: Hinged structure A

B

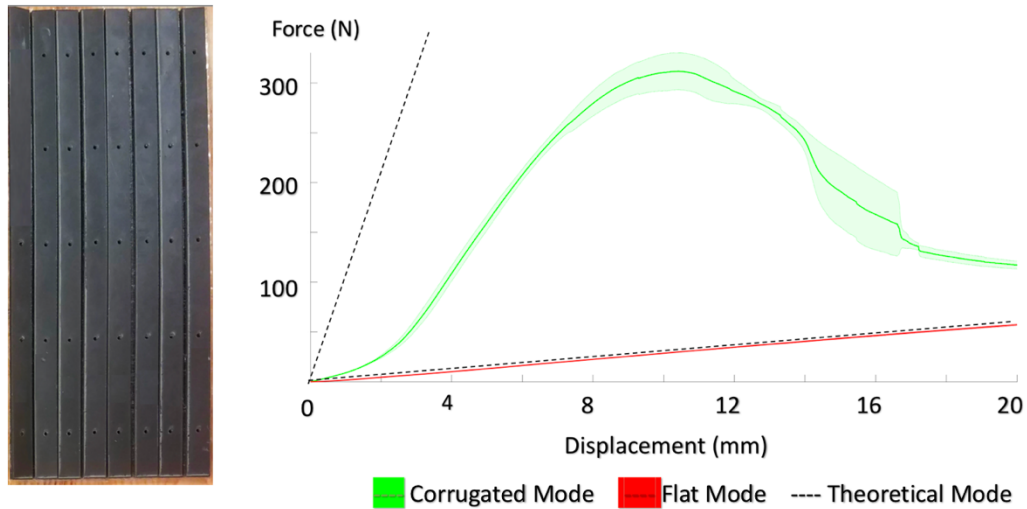


Figure 26: Hinged structure B

C

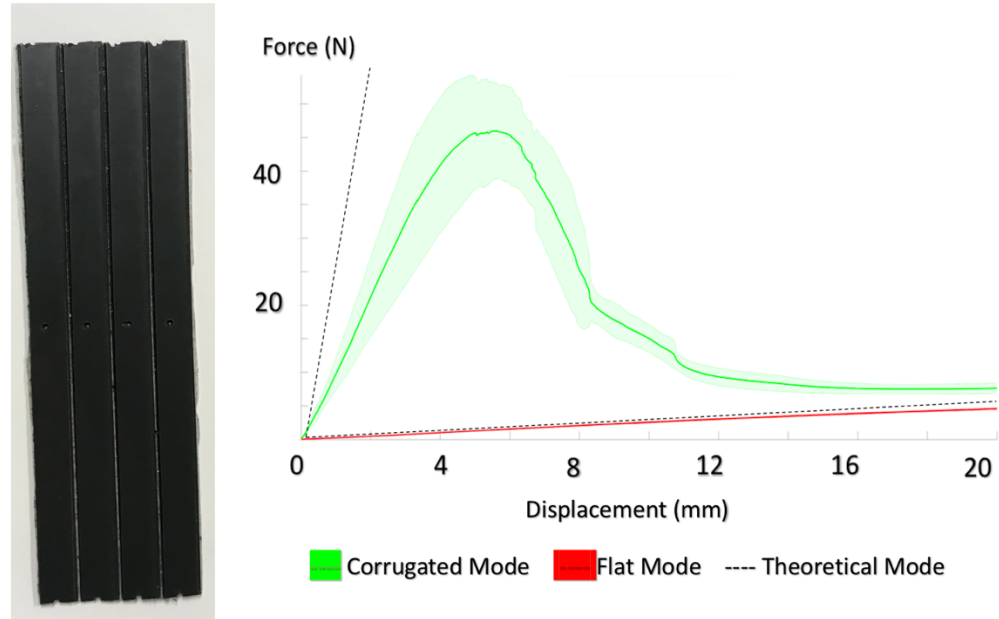


Figure 27: Hinged structure C

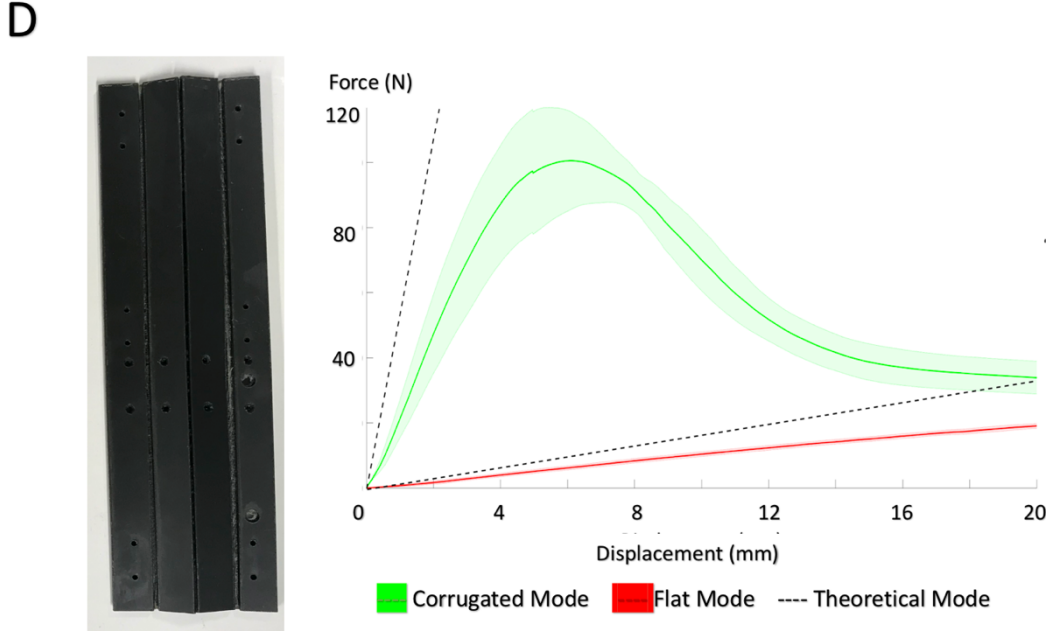


Figure 28: Hinged structure D

We experiment as in section 2.1.2, using three-point bending test to characterize the stiffness of each design.

Table 2: Hinged structure comparison

Hinged structure	w_1 (mm)	w_2 (mm)	t (mm)	θ (°)	n	Theoretical stiffness ratio	Experimental stiffness ratio	Maximum force
A	8	6.35	1.6	45	16	11.5	7.8	56
B	14.3	12.7	1.6	45	16	37.5	14	312
C	14.3	12.7	0.8	45	8	151	42	46
D	14.3	12.7	1.6	45	8	38.5	20.7	101

From the results, we can learn that the maximum force of the curve in sample B is the largest one among these four candidates, in addition we observed less delamination and twist during loading. However, it is hard to fix on the inner wrist because the width of the hinged structure is larger than the average width of the human wrist. Decreasing the width of each tab without changing the number of tabs, we obtain sample A with better stiffness but lower maximum load. In order to characterize the effect of tab numbers, sample D has the same lengths w_1 and w_2 compared with candidate B but half of the tabs. Sample C is half the thickness of the other samples to

determine the effect t plays in the stiffness.

From the results, we can see sample D has a larger maximum load compared to sample A and sample C. Although the theoretical stiffness ratio of sample C is much larger than the other two, its maximum load is much lower than the other two. Thus, we chose structure D for use in our brace.

3.3 Integrated Brace Testing

In order to investigate the behavior of the wrist brace, we did another set of experiments to test and simulate the performance in flat and corrugated mode. We used an aluminum bar whose cross section is $50 \times 30 \text{ mm}$ to simulate a human wrist and mounted in wrist brace on it. The constraining strap was tied around the bar and fixed the wrist joint and a L bracket was located at the bottom to stop the movement of the wrist brace in longitude direction.

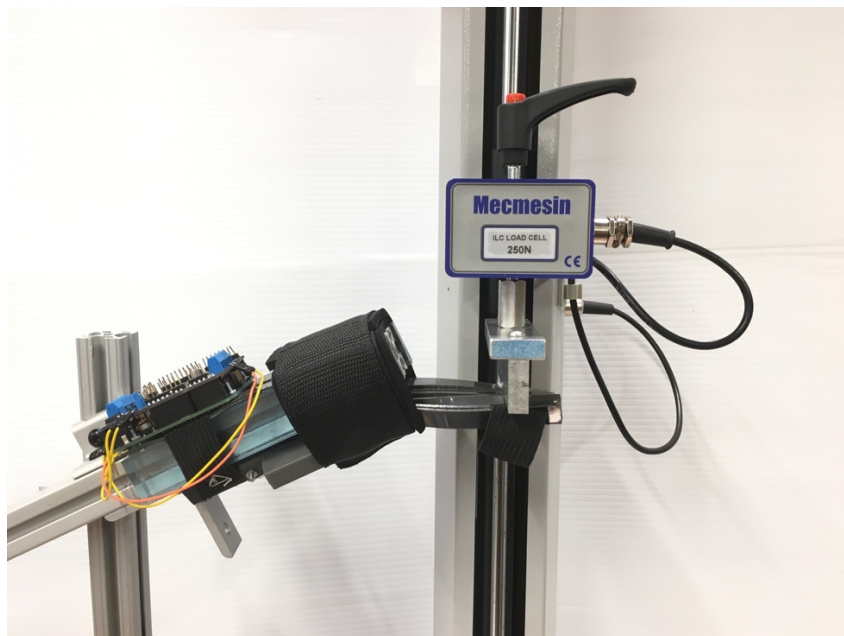


Figure 29: Integrated wrist brace test

As shown in Figure 29, a microcontroller is mounted on the top of the aluminum bar to control the motor. The wrist brace is deflected in 10° increments relative to the aluminum bar, from 0° to 70° , to simulate the total range of wrist flexion.

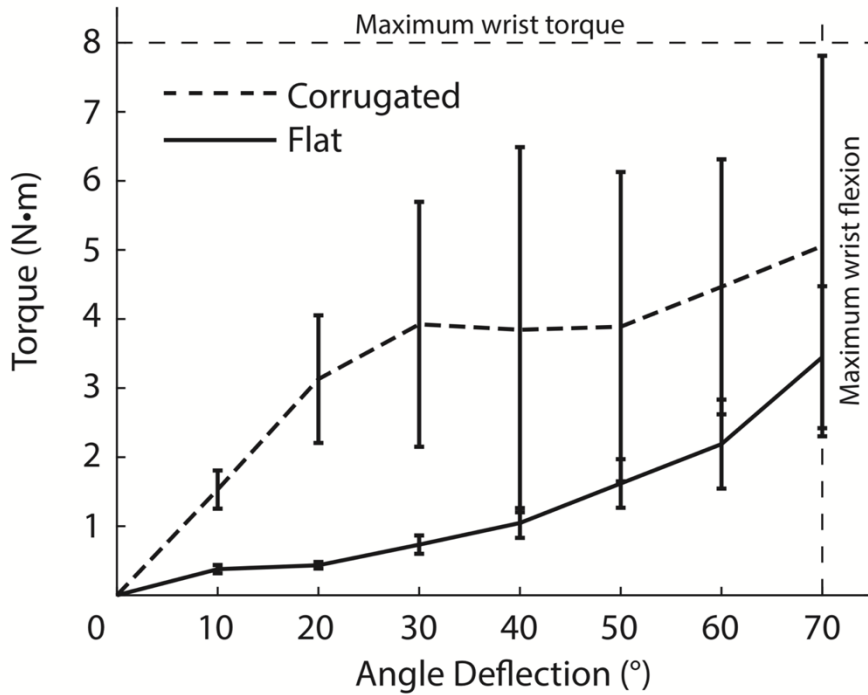


Figure 30: Torque exerted against the wrist brace as a function of angular deflection in both the flat mode and corrugated mode [17]

The results are shown in Figure 30, where the dashed line represents corrugated mode and the solid line represents flat mode. The results demonstrate that the hinged structure exerts $3.4 \text{ N} \cdot \text{m}$ torque at the largest angle 70 degrees in flat mode, still much lower the maximum wrist torque $8 \text{ N} \cdot \text{m}$, which means the average person could easily reach their maximum flexion [18]. In the corrugated mode, we can see the torque increases sharply with angle increase at the first 20 degrees, which is similar to the behavior we observed that hinged structure kept the shape. And the average torque leveled off at about $4 \text{ N} \cdot \text{m}$ when the deflection angle is 30 degrees and hinged structure begins to deform. We can also observe that the variation of samples is larger at this point, which we believed is due to delamination.

4 Discussion

This research introduces an origami approach to the orthopedic device based on self-folding technology. Actuators methods such as pneumatics, magnetics and temperature-based approaches require intermittent power to maintain a rigid state. Tendon actuation, however, is relatively efficient and consumes no external power to lock the structure.

For the integrated wrist brace, the method for mechanically coining the brace to the wrist brace needs to improve. One possibility is a slide belt which is able to control the length of strap precisely. Another way is changing the pattern of the hinged structure to other patterns which are more flexible in the flexible mode. Another challenge is that the tendon driven method requires motor not only to apply tension, but also to lock the hinged structure in the corrugated position. This may cause abrasion to the gears and reduce the life of motor. In the future work, a dedicated locking mechanism can be added to extend the life of the actuation unit.

The future design will still focus on improving wearability. The sharp edges of the hinged structure may have potential risks to hurt users' skin and will pinch palm and wrist even with glove protection. In addition, we will conduct further investigation into the wrist brace to make it easily wearable since the elastic bands and constraining strap will increase the complexity of wearing.

Base on the research and comparison above, there are some points we can conclude about the theoretical model. First, the theoretical model assumes the cross section is static. Based on the tests, bending effect still plays the most important part in the process, but we observed the torsion of elements under load cell leading additional displacement of the hinged structure by changing the corrugated angle. Future research needs to take this behavior into account and update the theoretical model. Second, we need to consider that the external forces are not uniformly distributed across the hinges but focused on the ridges, this may not be the same as the loading pattern when worn. Third, more complicated patterns may have better characteristics, such as the Miura-based pattern with orthogonal hinged structure leading to bidirectional transformation.

According to pattern and material experimental comparison, we determined the shape and material of the hinged structure and got the stiffness ratio is about 38.5 theoretically. But the model underperforms the theoretical calculation to some extent. We believe this is due to the additional deflection of segments during the test, which probably caused by torsion and sheering. These two effects not only reduce the bending modulus in corrugated mode, but also change the corrugated angle in each element. In the future work, we will take these effects into account.

REFERENCES

- [1] Fox, Steve. "Nine Real NASA Technologies in 'The Martian'." *NASA*. NASA, 13 Aug. 2015. Web. 31 July 2018.
- [2] Jenner, Lynn. "NASA's New Shape-Shifting Radiator Inspired by Origami." *NASA*. NASA, 31 Jan. 2017. Web. 31 July 2018.
- [3] Greicius, Tony. "Solar Power, Origami-Style." *NASA*. NASA, 21 July 2015. Web. 31 July 2018.
- [4] Sims, Josh. "Smart Buildings Are about Sustainability - but Also about Improving Lives." *South China Morning Post*. South China Morning Post, 09 Jan. 2017. Web. 31 July 2018.
- [5] Burton, Claire, Linda S. Chesterton, and Graham Davenport. "Diagnosing and managing carpal tunnel syndrome in primary care." *Br J Gen Pract* 64.622 (2014): 262-263.
- [6] Berger, M., et al. "The long-term follow-up of treatment with corticosteroid injections in patients with carpal tunnel syndrome. When are multiple injections indicated." *Journal of Hand Surgery (European Volume)* 38.6 (2013): 634-639.
- [7] Blausen, S. "com staff" Medical gallery of Blausen Medical 2014." *WikiJournal of Medicine* 1.2 (2014): 10.
- [8] Sasaki, Daisuke, Toshiro Noritsugu, and Masahiro Takaiwa. "Development of active support splint driven by pneumatic soft actuator (ASSIST)." *Robotics and Automation, 2005. ICRA 2005. Proceedings of the 2005 IEEE International Conference on*. IEEE, 2005.
- [9] Chou, Ching-Ping, and Blake Hannaford. "Static and Dynamic Characteristics of McKibben Pneumatic Artificial Muscles." *Proceedings of the 1994 IEEE International Conference on Robotics and Automation*, San Diego, CA. 1994.
- [10] Lenzi, Tommaso, et al. "NEUROExos: A variable impedance powered elbow exoskeleton." *Robotics and Automation (ICRA), 2011 IEEE International Conference on*. IEEE, 2011.
- [11] Blanc, Loïc, Alain Delchambre, and Pierre Lambert. "Flexible medical devices: review of controllable stiffness solutions." *Actuators*. Vol. 6. No. 3. Multidisciplinary Digital Publishing Institute, 2017.

- [12] Jafari, Amir, Nikos G. Tsagarakis, and Darwin G. Caldwell. "A novel intrinsically energy efficient actuator with adjustable stiffness (AwAS)." *IEEE/ASME transactions on mechatronics* 18.1 (2013): 355-365.
- [13] Cheng, Nadia G., et al. "Thermally Tunable, Self-Healing Composites for Soft Robotic Applications." *Macromolecular Materials and Engineering* 299.11 (2014): 1279-1284.
- [14] Loeve, Arjo J., et al. "Polymer rigidity control for endoscopic shaft-guide 'Plastolock'—a feasibility study." *Journal of Medical Devices* 4.4 (2010): 045001.
- [15] Kim, Yong-Jae, et al. "Design of a tubular snake-like manipulator with stiffening capability by layer jamming." *Intelligent Robots and Systems (IROS), 2012 IEEE/RSJ International Conference on*. IEEE, 2012.
- [16] Wenham, Martin. "Stiffness and flexibility." *200 science investigations for young students* (2001): 126.
- [17] Marcos Oliveira, Mengtao Zhao, Chang Liu, Samuel Felton, (2018) “Design of a variable stiffness wrist brace with an origami structural element” *Intelligent Robots and Systems (IROS), 2018 IEEE/RSJ International Conference on*. IEEE, 2018.
- [18] Morse, Jonathan L., et al. "Maximal dynamic grip force and wrist torque: The effects of gender, exertion direction, angular velocity, and wrist angle." *Applied Ergonomics* 37.6 (2006): 737-742.